

Supporting Materials (SM) for:

PVP-Regulated Synthesis of Ni-Fe Alloy Nanoparticles Anchored on N-Doped Graphene: Enhanced Kinetics and Stability for Ammonia Borane Hydrolysis

Yaling Zeng¹, Yuqian Ma, Yang Li, Zhendong Ouyang, Guanghua Cai, Xiaofei Li, Yunxiao Wen, Jian Yang*, Ximei Fan*

*Jian Yang, the Corresponding author, jyang10619@swjtu.edu.cn.

*Ximei Fan, Corresponding author, xmfan@swjtu.edu.cn.

Key Laboratory of Advanced Technologies of Materials (Ministry of Education), School of Materials Science and Engineering, Southwest Jiaotong University, Chengdu 610031, PR China

Density Functional Theory (DFT) computational methods

All density functional theory (DFT) calculations were performed using Materials Studio software. The generalized gradient approximation (GGA) with the Perdew-Burke-Ernzerhof (PBE) exchange-correlation functional was adopted to describe the electron-electron interactions. The cut-off energy for the plane-wave basis set was set to 400 eV. The convergence criteria for total energy and atomic forces were fixed at 2×10^{-6} eV and $0.01 \text{ eV} \cdot \text{Å}^{-1}$, respectively.

For model construction, a $4 \times 4 \times 1$ supercell of graphene with a vacuum layer of 15 Å was used to eliminate interlayer interactions. Pyridine N and pyrrole N doping models were established by substituting lattice C atoms with N atoms, and the doping positions were selected based on the lowest energy configuration to ensure structural stability. The Ni-Fe alloy cluster was anchored on the doped graphene surface, with the configuration optimized to the lowest energy state. Spin polarization was included in all calculations to account for the magnetic properties of transition metals. The adsorption energies of H₂O and AB molecules were calculated by comparing the total energy of the adsorbed system with the sum of the total energies of the isolated catalyst

model and adsorbate molecules. The work function was derived from the electrostatic potential difference between the vacuum level and the Fermi level.

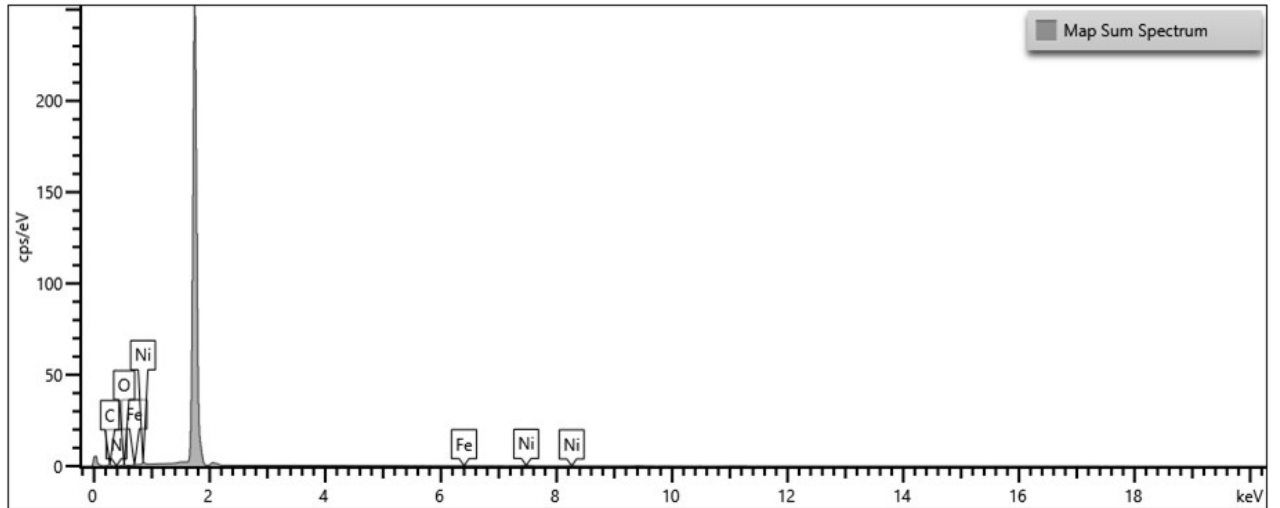


Fig. S1. The EDX spectrum of the $\text{Ni}_{3.5}\text{Fe}_{0.5}\text{-NG-1}$

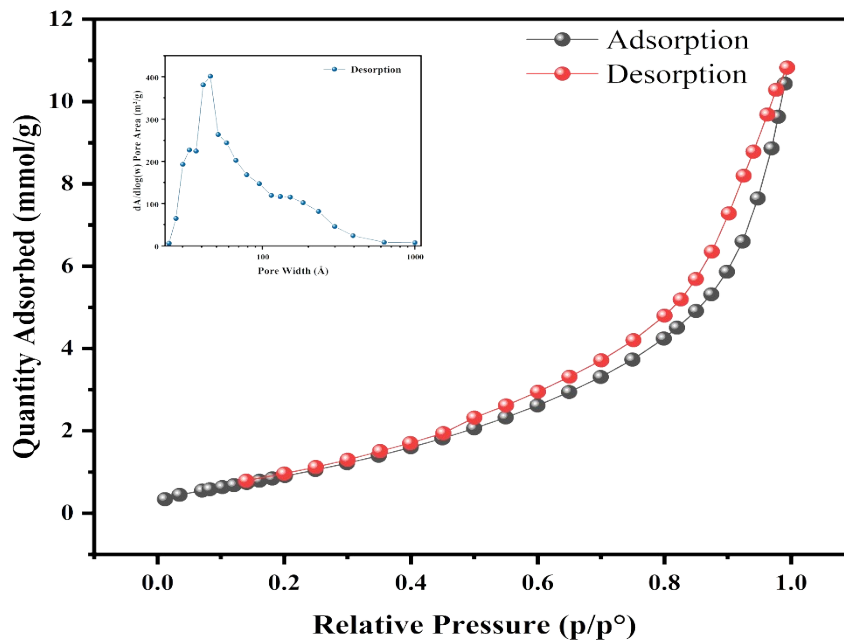


Fig. S2. Nitrogen adsorption-desorption isotherm of the $\text{Ni}_{3.5}\text{Fe}_{0.5}\text{-NG-1}$

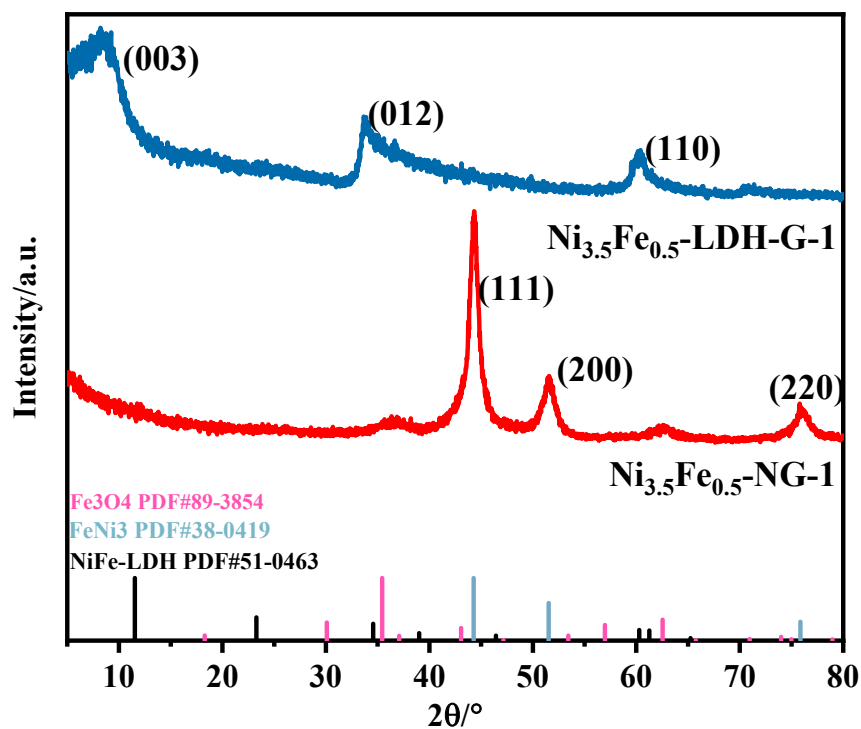


Fig. S3. The XRD patterns of $\text{Ni}_{3.5}\text{Fe}_{0.5}\text{-LDH-G-1}$ and $\text{Ni}_{3.5}\text{Fe}_{0.5}\text{-NG-1}$.

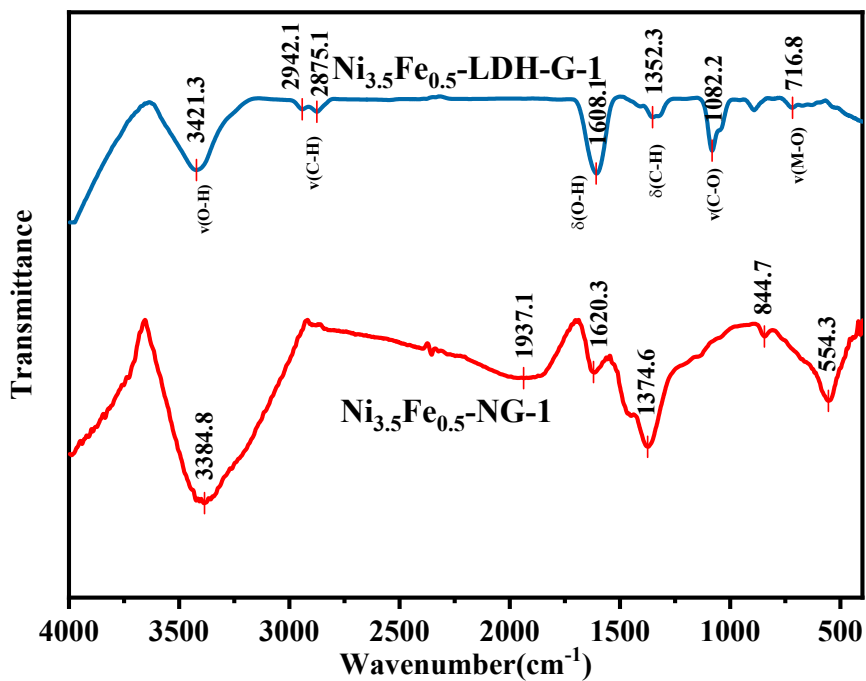


Fig. S4. The FTIR patterns of $\text{Ni}_{3.5}\text{Fe}_{0.5}\text{-LDH-G-1}$ and $\text{Ni}_{3.5}\text{Fe}_{0.5}\text{-NG-1}$.

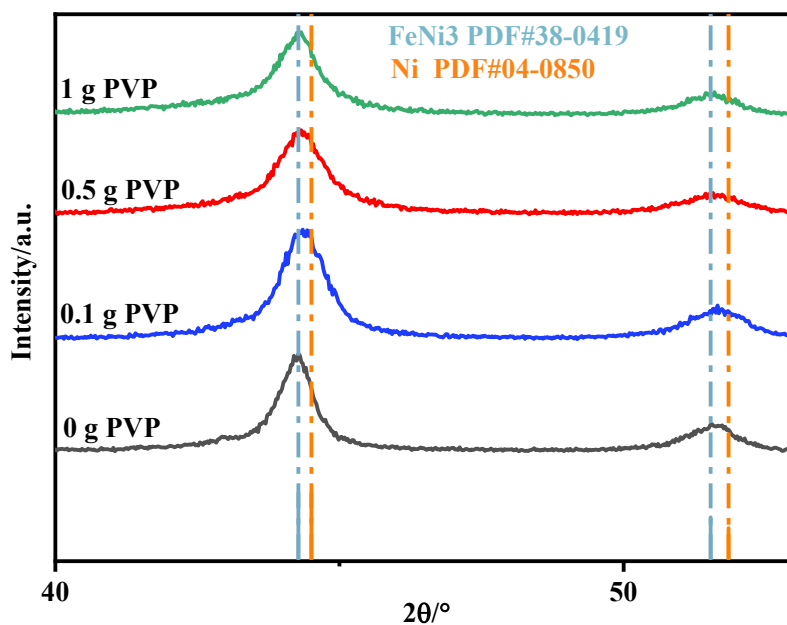


Fig. S5. The XRD patterns of Ni_{3.5}Fe_{0.5}-NG-1 with varied PVP amount.

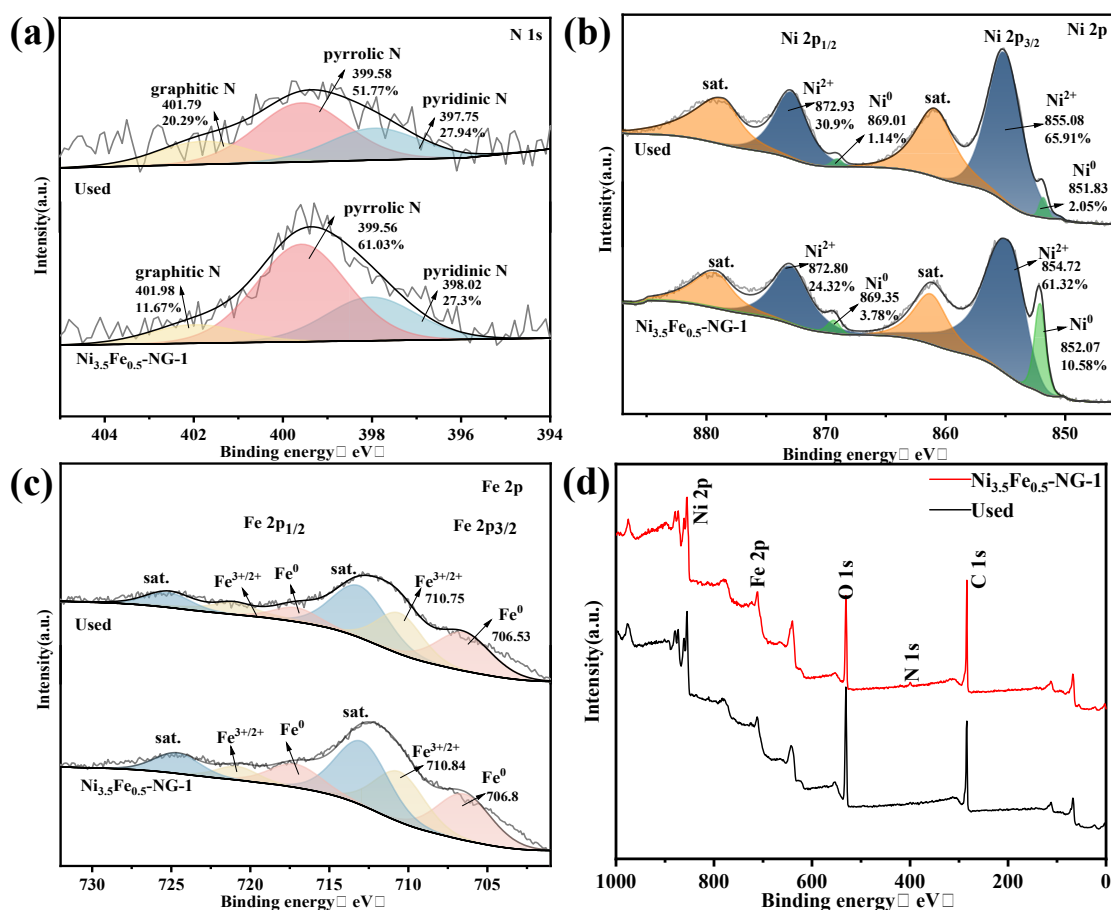


Fig. S6. XPS spectrum comparison of the Ni_{3.5}Fe_{0.5}-NG-1 catalyst and after (used) the recycling tests: (a) High-resolution N 1s spectrum, (b) High-resolution Ni 2p spectra, (c) High-resolution Fe 2p spectra, and (d) Full XPS spectrum.

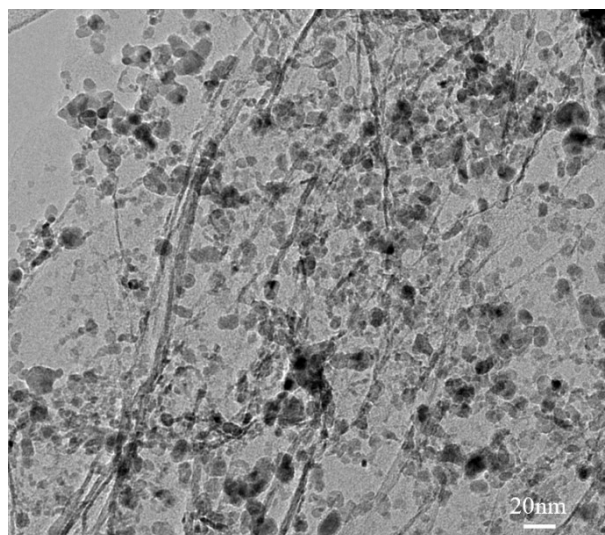


Fig. S7. TEM images of the $\text{Ni}_{3.5}\text{Fe}_{0.5}\text{-NG-1}$ catalysts after the recycling tests

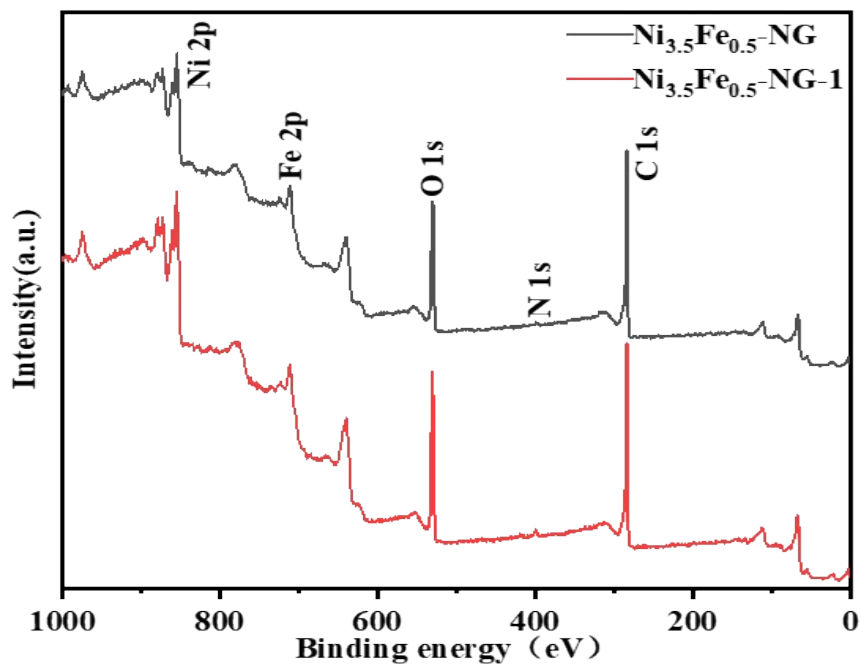


Fig. S8. Full XPS spectrum of $\text{Ni}_{3.5}\text{Fe}_{0.5}\text{-NG}$ and $\text{Ni}_{3.5}\text{Fe}_{0.5}\text{-NG-1}$ catalysts

Table S1. The actual molar ratios of Ni/Fe in the catalysts from the ICP-OES analysis.

Catalysts	molar ratio of Ni/Fe	
	feeding ratio	actual ratio
Ni _{3.5} Fe _{0.5} -NG	7:1	7.67:1
Ni _{3.5} Fe _{0.5} -NG-1	7:1	7.58:1

Table S2. The comparison of TOF and activation energies of various catalysts reported in the literature.

Catalysts	TOF (min ⁻¹) ¹⁾	Ea (kJ.mol ⁻¹)	Ref.
Ni _{1.2} Fe _{0.8} @CN-G	23.25	38.24	[1]
Ni/CNT	26.2	32.3	[2]
Ni/SiO ₂	13.2	34 ± 2	[3]
Ni/g-C ₃ N ₄	18.7	36	[4]
Ni	2.7	66	[5]
Ni NPs@3D-(N) GFs	41.7	31.6	[6]
Ni ₃ FeN	14.17	-	[7]
Ni-Co-P	58.4	-	[8]
CoCu/Ni	30.5	20.8	[9]
Ni/FeNiOx-25	55.6	39.18	[10]
Ni _{0.75} Cu _{0.25}	25.26	34.2	[11]
PVP-stabilized Co _{0.7} Ni _{0.3}	35.3	23.6	[12]
NiNPs/ZIF-8	35.3	-	[13]
PVP-stabilized Ni	12.1	62	[14]
NiCo ₂ O ₄ /Ti	50.1	17.5	[15]
Ni ₂ P NA/NF	42.3	44	[16]
Ni _{0.9} Mo _{0.1} /graphene	66.7	21.8	[17]
Cu ₂ Ni ₁ @MIL-101	20.9	32.2	[18]
NiMn-decorated CNFs	58.2	38.9	[19]
Ni _{0.13} Co _{0.87} P	47.5	41.8	[20]
Ni_{3.5}Fe_{0.5}-NG-1	55.8	44.2	This work

References

- [1] Cui C, Liu Y, Mehdi S, et al. Enhancing effect of Fe-doping on the activity of nano Ni catalyst towards hydrogen evolution from NH_3BH_3 [J]. *Applied Catalysis B: Environmental*, 2020, 265.
- [2] Zhang J, Chen C, Yan W, et al. Ni nanoparticles supported on CNTs with excellent activity produced by atomic layer deposition for hydrogen generation from the hydrolysis of ammonia borane [J]. *Catalysis Science & Technology*, 2016, 6(7): 2112-2119.
- [3] Metin Ö, Özkar S, Sun S. Monodisperse nickel nanoparticles supported on SiO_2 as an effective catalyst for the hydrolysis of ammonia-borane [J]. *Nano Research*, 2010, 3(9): 676-684.
- [4] Gao M, Yu Y, Yang W, et al. Ni nanoparticles supported on graphitic carbon nitride as visible light catalysts for hydrolytic dehydrogenation of ammonia borane [J]. *Nanoscale*, 2019, 11(8): 3506-3513.
- [5] Guo K, Li H, Yu Z. Size-Dependent Catalytic Activity of Monodispersed Nickel Nanoparticles for the Hydrolytic Dehydrogenation of Ammonia Borane [J]. *ACS Appl Mater Interfaces*, 2018, 10(1): 517-525.
- [6] Shang N Z, Zhou X, Feng C, et al. Synergetic catalysis of Ni-Pd nanoparticles supported on biomass-derived carbon spheres for hydrogen production from ammonia borane at room temperature [J]. *International Journal of Hydrogen Energy*, 2017, 42(9): 5733-5740.
- [7] Zhang X, Zhao Y F, Jia X D, et al. Silica-Protected Ultrathin Ni_3FeN Nanocatalyst for the Efficient Hydrolytic Dehydrogenation of NH_3BH_3 [J]. *Advanced Energy Materials*, 2018, 8(12): 7.
- [8] Hou C C, Li Q, Wang C J, et al. Ternary Ni-Co-P nanoparticles as noble-metal-free catalysts to boost the hydrolytic dehydrogenation of ammonia-borane [J]. *Energy & Environmental Science*, 2017, 10(8): 1770-1776.
- [9] Liao J Y, Lv F, Feng Y F, et al. Electromagnetic-field-assisted synthesis of Ni foam film-supported CoCu alloy microspheres composed of nanosheets: A high performance catalyst for the hydrolysis of ammonia borane [J]. *Catalysis Communications*, 2019, 122: 16-19.
- [10] Guan S Y, An L L, Chen Y M, et al. Enhancing Effect of Fe^{2+} Doping of Ni/NiO Nanocomposite Films on Catalytic Hydrogen Generation [J]. *Acs Applied Materials & Interfaces*, 2021, 13(36): 42909-42916.
- [11] Guo K, Ding Y, Luo J, et al. NiCu Bimetallic Nanoparticles on Silica Support for Catalytic Hydrolysis of Ammonia Borane: Composition-Dependent Activity and Support Size Effect [J]. *Acs Applied Energy Materials*, 2019, 2(8): 5851-5861.
- [12] Su X F, Li S F. PVP-stabilized Co-Ni nanoparticles as magnetically recyclable catalysts for hydrogen production from methanolysis of ammonia borane [J]. *International Journal of Hydrogen Energy*, 2021, 46(27): 14384-14394.
- [13] Wang C L, Tuninetti J, Wang Z, et al. Hydrolysis of Ammonia-Borane over Ni/ZIF-8 Nanocatalyst: High Efficiency, Mechanism, and Controlled Hydrogen Release [J]. *Journal of the American Chemical Society*, 2017, 139(33): 11610-11615.
- [14] Özhava D, Kiliçaslan N Z, Özkar S. PVP-stabilized nickel(0) nanoparticles as catalyst in hydrogen generation from the methanolysis of hydrazine borane or ammonia borane [J]. *Applied Catalysis B-Environmental*, 2015, 162: 573-582.

- [15] Liao J Y, Li H, Zhang X B, et al. Fabrication of a Ti-supported NiCo₂O₄ nanosheet array and its superior catalytic performance in the hydrolysis of ammonia borane for hydrogen generation [J]. *Catalysis Science & Technology*, 2016, 6(11): 3893-3899.
- [16] Tang C, Xie L S, Wang K Y, et al. A Ni₂P nanosheet array integrated on 3D Ni foam: an efficient, robust and reusable monolithic catalyst for the hydrolytic dehydrogenation of ammonia borane toward on-demand hydrogen generation [J]. *Journal of Materials Chemistry A*, 2016, 4(32): 12407-12410.
- [17] Yao Q L, Lu Z H, Huang W, et al. High Pt-like activity of the Ni-Mo/graphene catalyst for hydrogen evolution from hydrolysis of ammonia borane [J]. *Journal of Materials Chemistry A*, 2016, 4(22): 8579-8583.
- [18] Gao D D, Zhang Y H, Zhou L Q, et al. CuNi NPs supported on MIL-101 as highly active catalysts for the hydrolysis of ammonia borane [J]. *Applied Surface Science*, 2018, 427: 114-122.
- [19] Abutaleb A, Zouli N, El-Halwany M M, et al. Graphitic nanofibers supported NiMn bimetallic nanoalloys as catalysts for H₂ generation from ammonia borane [J]. *International Journal of Hydrogen Energy*, 2021, 46(71): 35248-35260.
- [20] Xiong C L, Zhang X W, Lei Y T, et al. One-pot synthesis of ultrafine Ni_{0.13}Co_{0.87}P nanoparticles on halloysite nanotubes as efficient catalyst for hydrogen evolution from ammonia borane [J]. *Applied Clay Science*, 2021, 214: 11.